Nuclear Science and Techniques (2025) 36:201
https://doi.org/10.1007/s41365-025-01776-3

Benchmark experiment system for ^{252}Cf spontaneous fission source using γ tagging

Yu-Ting Wei[1,2] · Chang-Lin Lan[1,2] · Bo Gao[1,2] · Xian-Lin Yang[1,2] · Gong Jiang[1,2] · Jia-Hao Wang[1,2] · Bo Xie[1,2] · Yang-Bo Nie[3] · Yan-Liang Chang[1,2] · Ge Zhang[1,2] · Fan Wu[1,2] · Kuo-Zhi Xu[1,2] · Shi-Long Liu[3] · Xi-Chao Ruan[3]

Received: 27 November 2024 / Revised: 19 January 2025 / Accepted: 28 January 2025 / Published online: 13 August 2025

Abstract
Benchmark experiments are indispensable for the development of neutron nuclear data evaluation libraries. Given the lack of domestic benchmarking of nuclear data in the fission energy region, this study developed a neutron leakage spectrum measurement system using a spherical sample based on the ^{252}Cf spontaneous fission source. The EJ309 detector (for high-energy measurements) and CLYC detector (for low-energy measurements) were combined to measure the time-of-flight spectrum using the γ tagging method. To assess the performance of the system, the time-of-flight spectrum without a sample was measured first. The experimental spectra were consistent with those simulated using the Monte Carlo method and the standard ^{252}Cf spectrum from ISO:8529-1. This demonstrates that the system can effectively measure the neutron events in the 0.15−8.0 MeV range. Then, a spherical polyethylene sample was used as the standard to verify the accuracy of the system for the benchmark experiment. The simulation results were obtained using the Monte Carlo method with evaluated data from the ENDF/B-VIII.0, CENDL−3.2, JEFF−3.3, and JENDL-5 libraries. The measured neutron leakage spectra were compared with the corresponding simulated results for the neutron spectrum shape and calculated C/E values. The results showed that the simulated spectra with different data libraries reproduced the experimental results well in the 0.15−8.0 MeV range. This study confirms that the leakage neutron spectrum measurement system based on the ^{252}Cf source can perform benchmarking and provides a foundation for evaluating neutron nuclear data through benchmark experiments.

Keywords ^{252}Cf · Neutron leakage spectrum · Benchmark experiment · Time-of-flight technique · Evaluated nuclear data · Spherical samples

1 Introduction

The dwindling reserves of fossil fuels and the desire to become less dependent on energy have recently propelled the need for safe and clean nuclear power to reach the forefront of power generation. Although current nuclear power plants perform well even beyond their expected lifetime, there is a desire for newer, safer, and more efficient designs [1, 2]. These factors have driven the development of novel nuclear power generation systems to meet the growing energy demand and protect the environment. However, accurate modeling simulations are required to analyze new core designs for reactors because of the significant capital costs associated with the construction of experimental reactors [3, 4]. One of the limiting factors of these simulations is the accuracy of the nuclear data inputs [5]. An important part of assessing data credibility is the benchmark experiment [5, 6].

Benchmark experiments provide a means of validating and improving nuclear data by comparing experimental results with theoretical predictions. Given their importance, China has been conducting neutron integral experiments

This work was supported by the National Natural Science Foundation of China (No. U2067205).

✉ Chang-Lin Lan
lanchl@lzu.edu.cn

[1] School of Nuclear Science and Technology, Lanzhou University, Lanzhou 730000, China

[2] Frontiers Science Center for Rare Isotopes, Lanzhou University, Lanzhou 730000, China

[3] Key Laboratory of Nuclear Data, China Institute of Atomic Energy, Beijing 102413, China

since 1960s [7]. Because of the half-life and production costs of the isotope neutron source, the D-T neutron generator has been primarily used for benchmark experiments, for examples those conducted by the China Academy of Engineering Physics (CAEP) [8–11] and the China Institute of Atomic Energy (CIAE) [12, 13]. In particular, the CIAE has developed an integral experimental platform to evaluate nuclear data in the fusion energy range [12–18]. However, fission reactors have been the primary source of nuclear energy for a long time. The accuracy of the neutron-evaluated data in the fission energy region is of great significance and application value for developing new reactors and designing miniaturized modular systems. Hence, it is essential to verify nuclear data within the fission energy range. It is well known that the $^{235}UO_2$ spectrum is a typical fission neutron spectrum. However, $^{235}UO_2$ requires neutron bombardment to initiate a fission reaction, which makes it unsuitable for this experiment. ^{252}Cf is a spontaneous fission source and its neutron energy spectrum is similar to that of $^{235}UO_2$, as illustrated in Fig. 1 [19]. Therefore, the ^{252}Cf source is generally used as a substitute for $^{235}UO_2$ in experiments that simulate the neutron spectrum generated by a fission reactor [19, 20]. Currently, experiments for measuring the leakage neutron spectrum based on a ^{252}Cf source primarily use the recoil proton method, which has a low resolution [21–24]. Additionally, there is a lack of benchmark results for the latest databases, such as the CENDL−3.2 library, because the experiment was conducted relatively early. Consequently, it is essential to conduct benchmark experiments using a ^{252}Cf source.

This study constructed the first leakage neutron spectrum measurement system for benchmark experiments based on the ^{252}Cf source using the time-of-flight (TOF) method in China. The proposed system utilizes γ tagging for coincidence detection. A spherical sample was used for the experiments, with the source positioned at the center of the sphere. The EJ309 liquid organic scintillator and Cs_2LiYCl_6:Ce (CLYC) detectors were used in conjunction to measure the neutron TOF spectrum, especially in the low-energy region. To assess the measurement capability of the system, the measured TOF spectrum without a sample was compared with the spectrum simulated using the Monte Carlo method and the ^{252}Cf standard spectrum in ISO:8529-1 [25]. Subsequently, experiments were conducted using a standard sample (a polyethylene sphere) to verify the reliability of the experimental system. The measured leakage neutron spectra were compared with the results simulated with the ENDF/B-VIII.0, CENDL−3.2, JEFF−3.3, and JENDL-5 libraries in terms of the spectrum shape and ratios of calculation to experiment (C/E) for the neutron flux [26–29]. This study provides a new domestic platform for benchmark experiments and is of great significance for checking and supplementing nuclear databases.

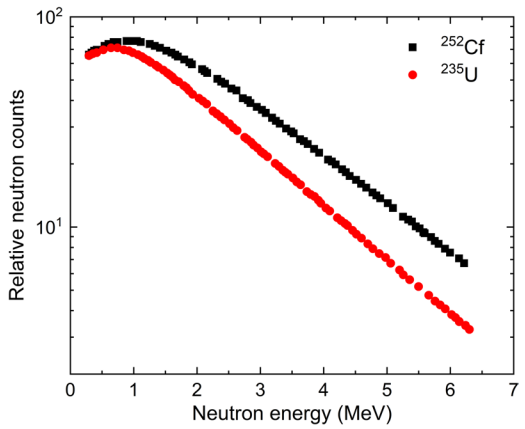

Fig. 1 Fission neutron spectra of ^{252}Cf and ^{235}U [20]

2 Experiment method

2.1 Experiment setup

The neutron emission rate of the ^{252}Cf source was greater than 10^5 n/s in the entire experiment period. The Silicon Carbide (SiC) detector for measuring fission fragments to obtain source neutron information and the take-off signal detector were positioned close to the source. The layout of the experimental platform is illustrated in Fig. 2. The experiments were performed using a spherical sample with the source located at the center of the sphere. This placement method is closer to practical application conditions, and it ensures that the nuclear reaction is carried out evenly in all directions and reduces the influence of the boundary effect. Thus, relevant information regarding the interaction between the neutrons emitted by the source at an angle of 4π and the sample can be effectively obtained. The EJ309 detector with a diameter and thickness of 2 in was purchased from SCIONIX Holland BV, and the energy resolution at $E_\gamma = 662$ keV was <7% FWHM. The CLYC detector (^{6}Li to > 95%) with a diameter and thickness of 2 in was manufactured by Radiation Monitoring Devices, Inc. (RMD). It is characterized by a high density and good energy resolution (<5% at $E_\gamma = 662$ keV) [30]. This detector is suitable for thermal neutron and low-energy neutron detection via the ^{6}Li(n, t)α reaction [31]. The EJ309 detector was positioned 200 cm away from the center of the ^{252}Cf fission source, and the CLYC detector was located 100 cm away. Both the ^{252}Cf source and the detector were placed 130 cm above the ground to reduce the impact of neutron scattering from the surrounding walls and ground.

All wave signals were acquired using a CAEN DT5730SB digitizer (14-bit, 500MS/s, 5.12MS/ch) because of its faster signal processing capability and the provided digital pulse

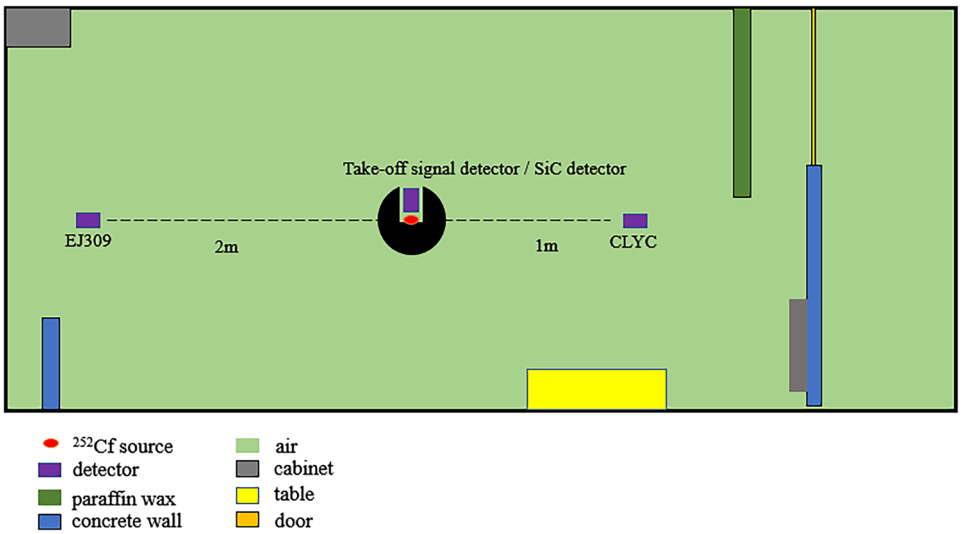

Fig. 2 (Color online) Experimental arrangement for measuring the neutron leakage time-of-flight (TOF) spectrum

processing-pulse shape discrimination (DPP-PSD) software for online pulse shape discrimination (PSD) analysis. When the online analysis is insufficient, the digitized signals can be stored for offline processing [32].

2.2 Take-off signal tagging

The measurement principle of the TOF method is expressed in Eq. (1).

$$t = \frac{72.306L}{\sqrt{E}} \tag{1}$$

where t is the time-of-flight (ns), E is the neutron energy (MeV), and L is the flight-path distance (m). In the case of a fixed distance between the fission source and detector, the only variable is the time from the fission event to the neutron recorded by the neutron detector. Hence, determining the take-off signal is crucial. For this measurement, the accompanying γ-rays emitted by fission were used to determine the timing of the fission events. Because the take-off signal detector was close to the neutron source in the experiment, the flight time of the γ-ray to this detector was practically negligible compared to that of the neutron to the second detector. The feasibility of this approach was demonstrated by Blain et al. who reproduced the prompt fission neutron spectrum (PFNS) using the γ tagging method [33]. Owing to the advantages of a fast response time, high detection efficiency for γ-rays, and low detection sensitivity for neutrons, the BaF_2 detector with a diameter and thickness of 1 in was used to identify the take-off time in this measurement.

2.3 Coincidence model

The coincidence mode allows for the setting of a variable length time window. When a pulse is detected in one channel, the window is initiated; if a pulse is detected in the other channel during this period, a coincidence event is logged. The possible types of coincidences that may have occurred during the experimental process are listed in Table 1. Detector 1 was used to measure the take-off signal, whereas detector 2 measured the flight termination signal.

In addition to the γ-n events, the γ-γ coincidence and accidental coincident events still existed in this measurement. Because γ-rays travel at the speed of light, the flight time difference between two coincident γ-rays can reach 6 ns. Regardless of the detector at which they arrive, γ-rays arrive first, following the corresponding fission event. As shown in Fig. 3, all γ–γ coincidence events still fall within the gamma peak region. This initial peak in the TOF spectrum represents double γ-ray events: either a single photon scattered between the detectors or two correlated prompt photons. Therefore, the neutron peak is not affected by the γ–γ coincidence events. Accidentally

Table 1 Coincident detection mechanisms in the two detectors found in this measurement

Particle in detector 1	Particle in detector 2	Correlation mechanism
γ	γ	Correlated γ from the same fission event
γ	γ	Single γ scattered between detectors
γ	n	Prompt gamma detected in detector 1, prompt neutron detected in detector 2
γ	n	Prompt gamma detected in detector 1, scatter neutron detected in detector 2
other	other	Accidentally coincident events

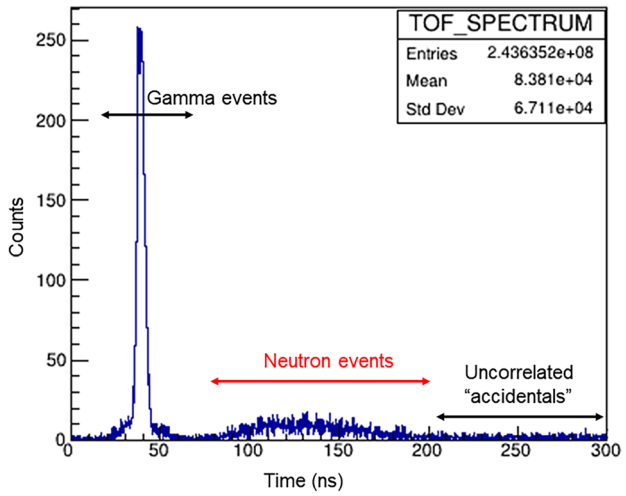

Fig. 3 The TOF spectrum was measured from a ^{252}Cf fission source using EJ309. The Gamma peak seen on the left contains coincident gamma detections. Events involving neutrons form a "hump" produced by the range of arrival times for neutrons of different energies. The initial flight time needs to be redetermined based on γ peak information

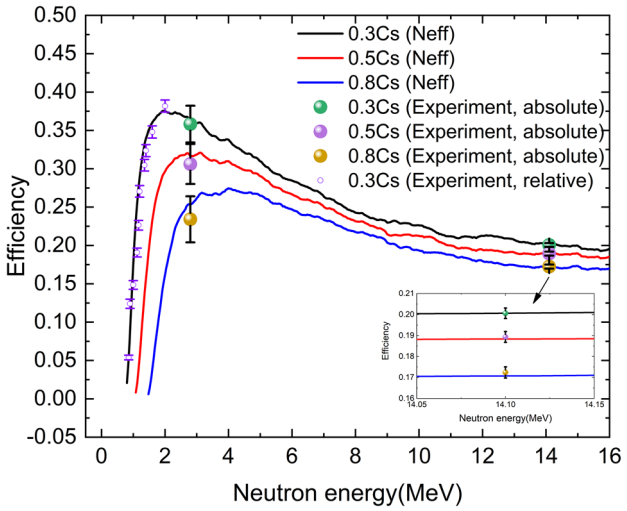

Fig. 4 (Color online) Detection efficiency of EJ309 calculated by the NEFF code compared with experimental values in different thresholds

coincident events can be corrected by taking the average count of the bins that represent the arriving coincidences.

2.4 Neutron detection Efficiency determination

The neutron detector efficiency is a vital parameter that directly affects the accuracy of the simulated TOF spectra. Therefore, for the EJ309 neutron detector, the neutron detection efficiency was accurately obtained using the Monte Carlo code NEFF under different detection thresholds [34]. The reliability of the calculated efficiency curves was experimentally calibrated. The absolute efficiencies of the EJ309 detector were determined by the D-D and D-T neutron generators in CIAE using the TOF method, and the relative detection efficiencies were measured by the ^{252}Cf source. The experimental detection efficiencies are in good agreement with the calculated results of the NEFF code in the range of uncertainty, as shown in Fig. 4.

The detection efficiency curve of the CLYC detector was simulated using the MCNP-4C code. This method has been previously confirmed as feasible, for example, in [35]. The relative detection efficiencies were measured by the ^{252}Cf source using the TOF method. As shown in Fig. 5, the calculated results are consistent with the experimental results within the uncertainty range.

3 Data processing

After the neutron TOF spectrum was measured, it was processed according to the process flow as shown in Fig. 6 to obtain pure and reliable neutron events. Subsequently, the experimental uncertainty was determined based on the measurement process. The pulse shape discrimination and background correction are described in this section.

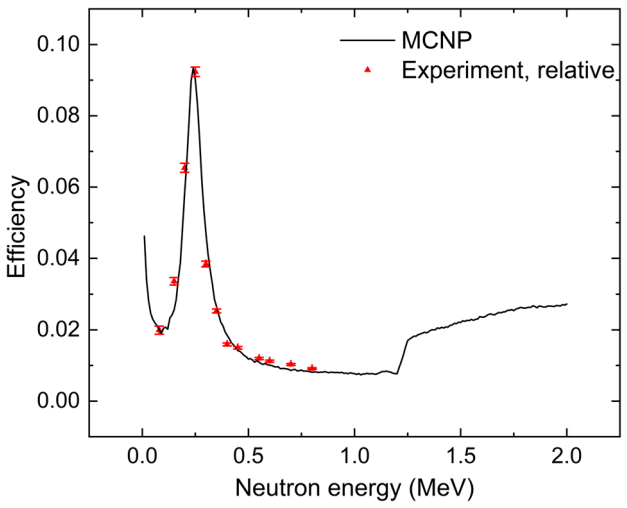

Fig. 5 The detection efficiency curve of the CLYC detector simulated by MCNP-4C compared with experimental values

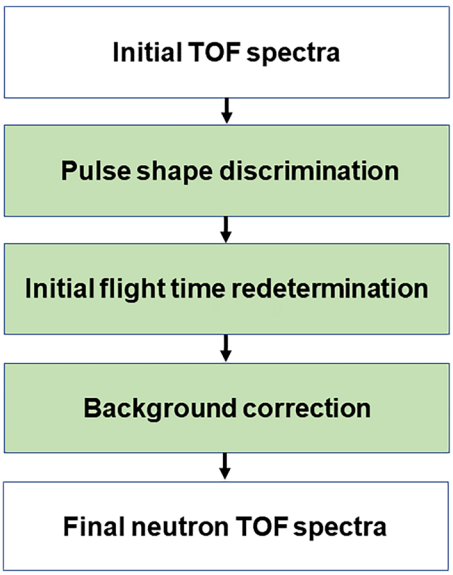

Fig. 6 Data processing flow of the measured TOF spectra

3.1 Pulse shape discrimination

To distinguish between the neutrons and γ-ray pulses, a pulse shape discrimination (PSD) technique was performed using the charge integration method [36, 37]. In this experiment, when the TOF spectrum based on ^{252}Cf was measured, the PSD information was obtained by analyzing the data through the waveform acquisition method. The neutron TOF spectra were derived by selecting neutron events, as shown in Fig. 7.

3.2 Background correction

Background correction is crucial for processing the data of the TOF spectrum. This study had three background components: time-independent background, time-dependent neutron background, and time-dependent γ background. The easiest determination was that of the time-independent background, which arose from random events that did not correlate with the fission process occurring in the measurement window. This is shown in Fig. 3, where the count rate flattens at a long TOF spectrum. This background component was eliminated by subtracting the count rate from each channel in the average 210–300 ns region.

The second background component, the time-dependent γ background, originated primarily from the γ decay of fission fragments [38]. This background is not present in the EJ309 and CLYC detectors because PSD can remove the background from γ-rays.

The third background component is the time-dependent neutron background. This affected both the EJ309 and CLYC detectors and primarily originated from prompt fission neutrons scattering off the surrounding structures and scattering back to the neutron detectors. To determine the impact of neutron scattering, the background TOF spectrum was experimentally measured using shadow cones, as shown in Fig. 8. The effect/background ratio measured by the EJ309 detector was greater than 7, and the CLYC detector demonstrated a ratio exceeding 4. Once all these background components were corrected from the experimental signal, a pure TOF spectrum was obtained.

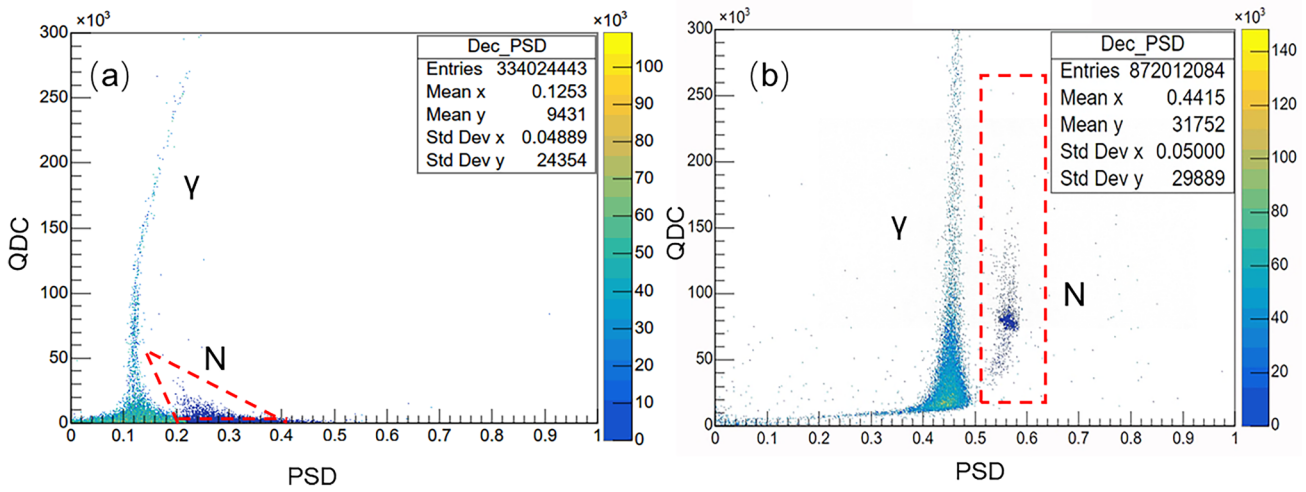

Fig. 7 (Color online) 2D plots of pulse shape discrimination (PSD) versus QDC for the (a) EJ309 and (b) CLYC detectors of the neutron signals from a ^{252}Cf source. The graph shows the ability of detectors to distinguish these two types of radiation. The areas framed by red lines are neutron events

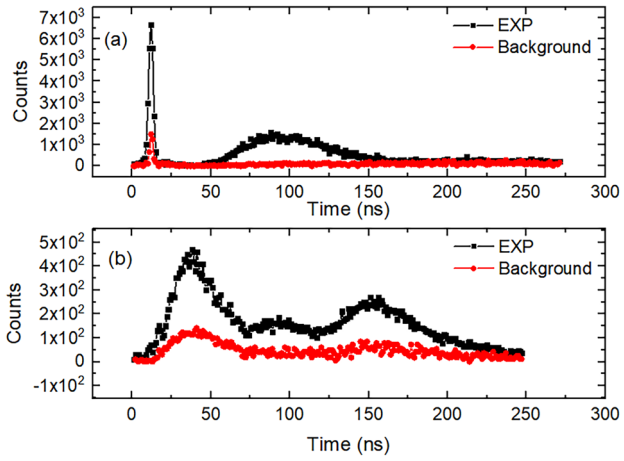

Fig. 8 Background spectra measured by the (a) EJ309 detector and (b) CLYC detector

3.3 Uncertainties analysis

The uncertainties of the present experiment mainly come from the statistical and systematic uncertainty, as presented in Table 2. Statistical uncertainty includes the uncertainties of neutron counting and ^{252}Cf source neutron counting (used for data normalization). The systematic uncertainty is caused by angle ambiguity and relative error of the detector efficiency.

It can be observed that the neutron counting uncertainty is the most significant contributor to the overall uncertainty. For more than 80% of the data points, the statistical uncertainties in the neutron counts measured by the EJ309 detector in the range of 0.8−8.0 MeV were below 3%. Meanwhile, the uncertainties in neutron counts measured by the CLYC detector in the range of 0.15−0.8 MeV were approximately 8%. During the experiment, source neutron counts were obtained by monitoring the information of the fission fragment ^{252}Cf. Therefore, the uncertainty of the ^{252}Cf source neutron counting arose from fission fragment counting, which was 1.31% and 1.22%, respectively, in the two experiments. The angular uncertainty induced by deviations in the positioning of the samples and detectors was relatively small at approximately 0.1%. The uncertainty in the detection efficiency stemmed from discrepancies between the experimental and simulated results.

4 Results

4.1 Capability of the neutron spectrum measurement system

To verify the capability of the constructed TOF spectrum measurement system, measurements were first performed without samples.

4.1.1 Time-of-flight spectrum of the EJ309 detector without sample

After the data were processed as shown in Fig. 6, the final TOF spectrum was obtained, as shown in Fig. 9. The TOF spectrum simulated by MCNP-4C was compared with the experimental spectrum. The TOF spectrum simulated

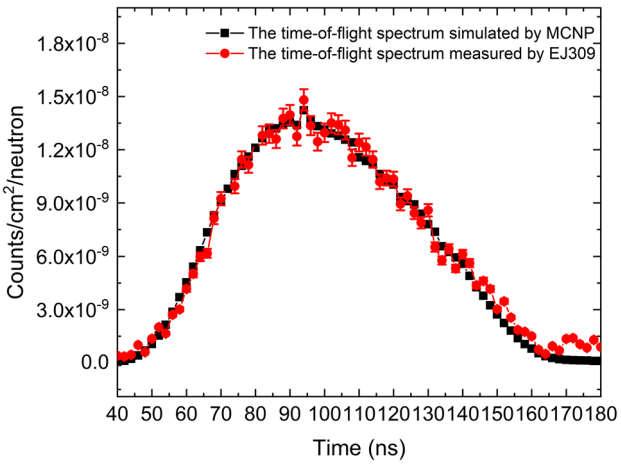

Fig. 9 TOF spectrum measured by the EJ309 detector without sample compared with the simulated spectrum

Table 2 Uncertainties in TOF spectra measurements

Uncertainty components		TOF spectra without sample		TOF spectra with polyethylene standard sample	
		50–161 ns (0.8–8 MeV)	80–162 ns (0.1–0.8 MeV)	50–161 ns (0.8–8 MeV)	80–162 ns (0.1–0.8 MeV)
Statistical	neutron counting	2.51%	8.16%	2.40%	7.76%
	^{252}Cf source neutron counting	1.31%	1.31%	1.22%	1.22%
Systematic	angle ambiguity	0.1%	0.1%	0.1%	0.1%
	neutron detector efficiency	2.88%	3.15%	2.88%	3.15%
Total		4.04%	8.85%	3.94%	8.46%

showed good agreement with the measured spectrum in the 50–162 ns (0.8–8 MeV) range.

To assess the measurement accuracy of the TOF spectrum platform, the data were converted from the time domain to the energy domain using Eq. (1) and compared with the ^{252}Cf standard spectrum from ISO:8529-1. Owing to the deviation between the Maxwellian standard spectrum at a nuclear temperature of 1.42 MeV and the ^{252}Cf experimental spectrum, the standard spectrum was folded using the detection efficiency curve [39]. Figure 10 shows the effect of detector efficiency on the ^{252}Cf standard spectrum. Then, the experimental spectrum was compared with the folded standard spectrum, as shown in Fig. 11. The experimental spectra were consistent with the standard spectrum in the uncertainty range. Although good consistency was observed across most of the measured data, the high-energy bins of the spectrum were somewhat higher than expected, and the peak value moved toward the high-energy region. This conclusion is similar to that of Becchetti, Blainand, and Alexander [20, 40, 41]. Two reasons may explain this. First, this could be a systematic error stemming from the assumption that prompt neutrons and γ-rays are simultaneously produced at the same moment in the measurement system. Typically, prompt fission γ-rays are emitted within a nanosecond after the fission event. However, some fission fragments exist in metastable states that decay over longer periods [42]. For short flight times, even minor delays in the gamma emission times would lead to an overestimation of the neutron energy, resulting in an overpopulation of the high-energy bins [41]. Second, the ^{250}Cf in the Cf source also has a certain probability of spontaneous fission, as presented in Table 3. When the ^{252}Cf source was produced, the atomic number ratio of ^{252}Cf to ^{250}Cf was approximately 5:1, the decay constant

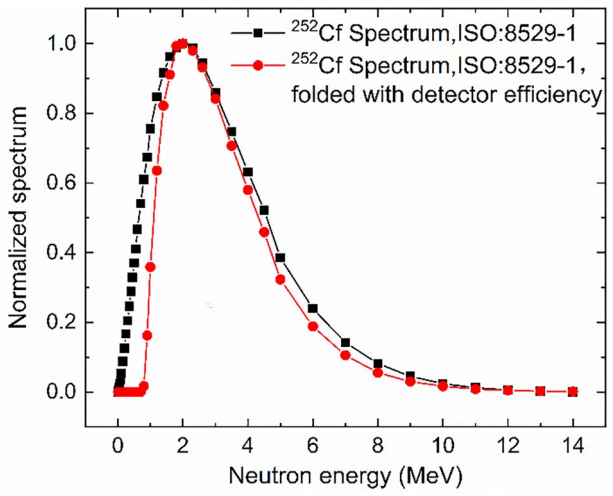

Fig. 10 Effect of the detector efficiency on the ^{252}Cf standard spectrum. Both curves have been normalized to a value of 1 at 2 MeV

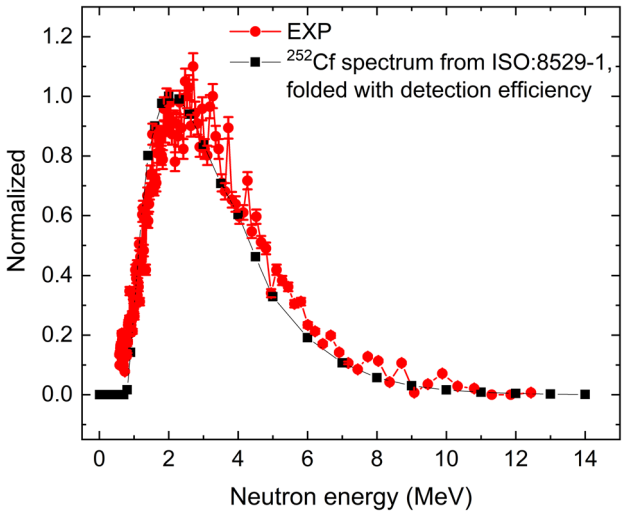

Fig. 11 ^{252}Cf experimental energy spectrum measured by the EJ309 detector compared with the standard ^{252}Cf energy spectrum from ISO:8529-1 folded with detection efficiency

ratio was approximately 5:1, and the spontaneous fission branching ratio was approximately 40:1. Therefore, at the initial stage, the contribution of ^{250}Cf to the neutron emissivity was approximately 0.1%, which had a small effect on the energy spectrum of ^{252}Cf. However, the contribution to the neutron emissivity of ^{250}Cf gradually increased with time. This also affected the energy spectrum of ^{252}Cf.

4.1.2 Time-of-flight spectrum of CLYC detector without sample

After the data were processed as shown in Fig. 6, the final TOF spectrum was obtained, as shown in Fig. 12. The TOF spectrum simulated by MCNP-4C showed the same trend as the measured spectrum in the 80–187 ns (0.15−0.8 MeV) range.

Similarly, the TOF spectrum was converted from the time domain to the energy domain to yield the final PFNS. In Fig. 13, the ^{252}Cf standard spectrum from ISO:8529-1 is folded with the efficiency curve of the CLYC detector. The final comparison results showed that the shape of the experimental spectrum matched the peak of the ISO:8529-1 spectrum in the low-energy regions. However, the TOF spectrum in the 1.2–5 MeV range appeared slightly lower than expected. In contrast, those in the range over 5.0 MeV were higher than the standard spectrum, with the peak value moving toward the high-energy region. This is related to the CLYC detector that detects neutrons using nuclear reactions. The neutron recorded by the CLYC detector is mainly caused by the following reactions [37]: (1) ^{6}Li(n, t)α (Q-value = 4.783 MeV) thermal neutron reaction; (2) ^{6}Li(n, t)α fast neutron reaction; (3) ^{35}Cl(n, p)^{35}S (Q = 0.615 MeV) fast neutron

Table 3 Decay data of Cf isotopes in the Cf source and daughter nuclides

Isotope	Half life (a)	Decay constant (s^{-1})	Spontaneous fission probability (%)	Average neutron number of each fission
^{252}Cf	2.645	8.304×10^{-9}	3.092	3.767
^{251}Cf	898	2.445×10^{-11}	0	–
^{250}Cf	13.08	1.679×10^{-9}	0.077	3.52
^{248}Cm	3.48×10^{5}	6.311×10^{-14}	8.39	3.16

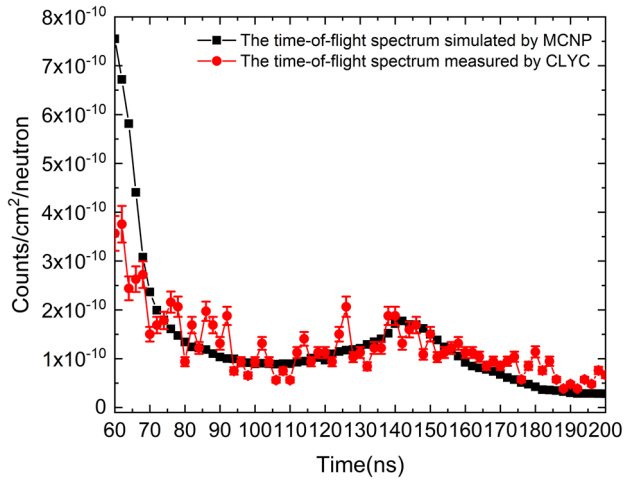

Fig. 12 TOF spectrum measured by the CLYC detector without sample compared with the simulated spectrum

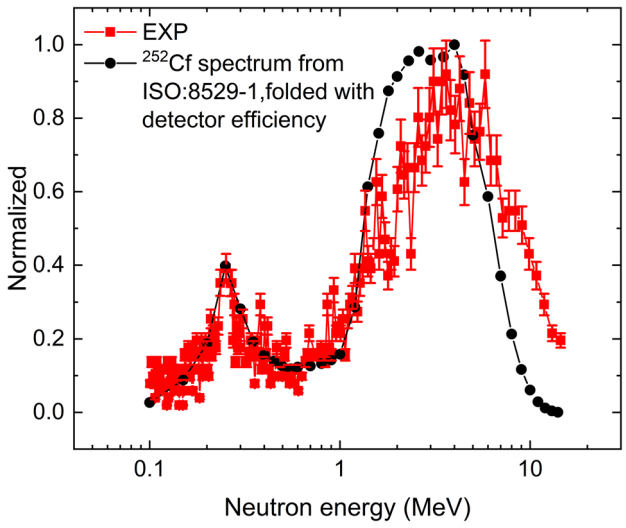

Fig. 13 ^{252}Cf experimental energy spectrum obtained by the CLYC detector compared with the standard ^{252}Cf energy spectrum from ISO:8529-1 folded with detection efficiency

reaction and (4) ^{35}Cl(n, α)^{32}P ($Q = 0.937$ MeV)fast neutron reaction. The reaction cross-sections are shown in Fig. 14.

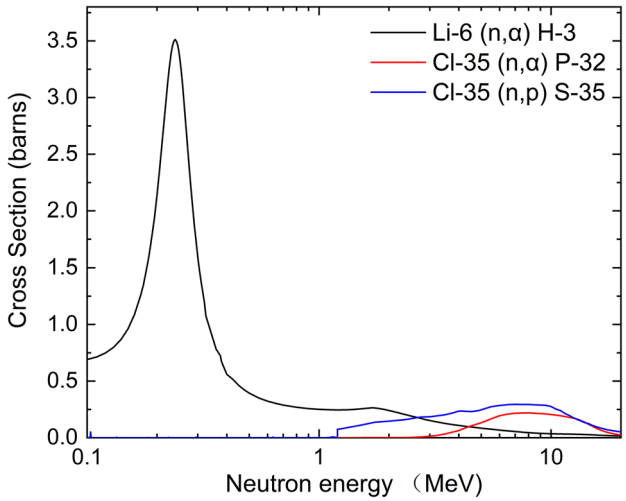

Fig. 14 Cross-sections of the different reactions considered. It is to be noted that the cross section value for this neutron absorption reaction at $E_n \sim 0.025$ eV is approximately 940 b (not shown in the figure) [43]

It can be seen that the ^{6}Li(n, t)α reaction is mainly effective when measuring neutrons in the 0.1–1 MeV range, whereas ^{35}Cl(n, p)^{35}S and ^{35}Cl(n, α)^{35}P are significant for neutron energies higher than 1.2 MeV. Moreover, a quenching factor exists in the ^{35}Cl fast neutron reactions [37]. For example, 2.5 MeV neutrons are detected by the ^{35}Cl(n, p)^{35}S reaction (2.5 MeV neutrons have a cross section of 0.19 b), as a single energy peak at 2.5 MeV and the Q-value of the reaction, multiplied by a proton quenching factor equal to 0.9, is 2.8 MeV. As a result, the shift in the peak position at energies greater than 1.4 MeV leads to poor agreement between the experimental and standard spectra in the high-energy region. However, this also proves that CLYC (95% ^{6}Li) is more suitable for measuring TOF spectra in the low-energy region.

4.2 Verification of the benchmark experiment reliability with the standard sample

The elastic scattering of neutrons and hydrogen (n–p scattering) was considered as the standard cross-section.

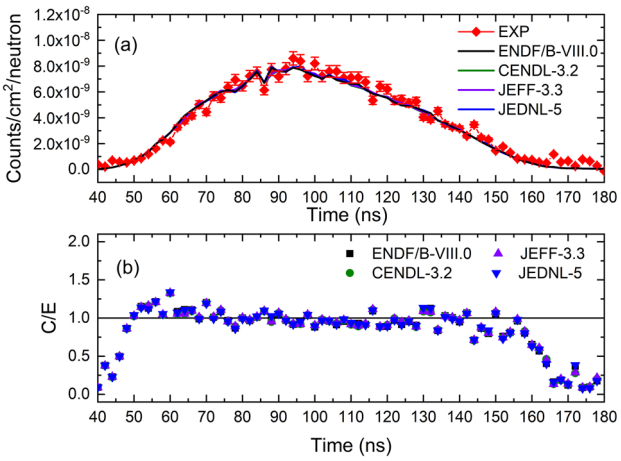

Fig. 15 Comparison of the measured and simulated neutron leakage TOF spectra with a polyethylene standard sample in the 0.8–8.0 MeV range. (a)The neutron leakage spectrum simulated by MCNP-4C was compared with those measured with EJ309. (b) C/E variation between the simulated spectra and measured spectrum

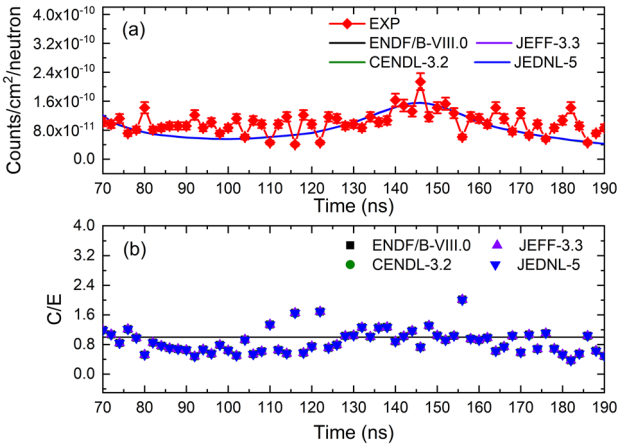

Fig. 16 Comparison of the measured and calculated neutron leakage TOF spectra with a polyethylene standard sample in the 0.15–0.8 MeV range. (a) The neutron leakage spectrum simulated by MCNP-4C was compared with those measured with CLYC. (b) C/E variation between the simulated spectra and measured spectrum

Therefore, a benchmark experiment using polyethylene ($\Phi = 12\,\mathrm{cm}$) was conducted to ensure the reliability of the system.

The measured spectra were compared with the spectra simulated using the MCNP-4C code with ENDF/B-VIII.0, CENDL-3.2, JEFF-3.3, and JENDL-5 libraries, as shown in Figs. 15 and 16. The ratios of the calculation to experiment (C/E) obtained by integrating the neutron peaks are listed in Table 4. The measured neutron leakage spectra were consistent with the simulated results obtained using MCNP-4C. In the 0.8–8 MeV (t = 50–162 ns) range, the calculated results were underestimated by approximately 5%, and the uncertainty was less than 3.94%. In the 0.15–0.8 MeV range (t = 80–187 ns), the calculated results were underestimated by approximately 13%, and the uncertainty was less than 8.46%. Therefore, the experimental results agree well with the simulated results in the range of 0.15–8.0 MeV. This indicates that the experimental system and data processing method used in this study are reliable, which ensures the reliability of conducting other sample data measurements.

5 Summary

In this study, the first neutron leakage spectrum measurement system for benchmark experiments in China based on the ^{252}Cf source with spherical samples using the TOF method was constructed. By utilizing the EJ309 and CLYC detectors, the platform reduced the energy limit of benchmarking based on ^{252}Cf sources. The experimental spectrum without the sample showed excellent consistency compared with the TOF spectrum simulated by the Monte Carlo method and the standard spectrum of ISO:8529-1, proving that the system was able to measure the neutron spectrum in the range of 0.15–8.0 MeV. Subsequently, the neutron leakage TOF spectra of the polyethylene standard sample were measured and the simulated spectra were obtained by MCNP-4C using the evaluated nuclear data from the ENDF/B-VIII.0, CENDL-3.2, JEFF-3.3, and JENDL-5 libraries. The essential characteristic properties of the neutron leakage spectra were well reproduced by these simulations, with deviations of less than 3.94% in the 0.8–8 MeV region and approximately 8.46% in the 0.15–0.8 MeV region. This demonstrates the ability of the leakage neutron spectrum system based on the ^{252}Cf source using spherical samples to perform benchmark tests and proves the feasibility of the entire set of benchmark experimental methods. This study provides a research foundation for evaluating key nuclear data based on the fission spectrum.

Table 4 C/E values of the spectra integrated over two energy regions

Neutron energy (MeV)	C/E value			
	ENDF/B-VIII.0	CENDL−3.2	JEDNL−5.0	JEFF−3.3
0.8−8.0	0.959±0.038	0.956±0.038	0.960±0.038	0.959±0.038
0.15−0.8	0.880±0.074	0.879±0.074	0.878±0.074	0.880±0.074

Acknowledgements The authors thank the operational staff of the Cockcroft-Walton accelerator at the China Institute of Atomic Energy for their support during the efficiency calibration experiments.

Author Contributions All authors contributed to the study conception and design. Funding acquisition, supervision, and writing were performed by Chang-Lin Lan, Yang-Bo Nie, Shi-Long Liu, and Xi-Chao Ruan. Material preparation, data collection, and analysis were performed by Yu-Ting Wei, Bo Gao, and Kuo-Zhi Xu. Investigation was performed by Gong Jiang, Jia-Hao Wang, Bo Xie, Yan-Liang Chang, Ge Zhang, and Fan Wu. The first draft of the manuscript was written by Yu-Ting Wei and all authors commented on previous versions of the manuscript. All authors read and approved the final manuscript.

Data availibility statement The data that support the findings of this study are openly available in Science Data Bank at https://cstr.cn/31253.11.sciencedb.cast.00025 and https://doi.org/10.57760/sciencedb.cast.00025.

Declarations

Conflict of interest The authors declare that they have no Conflict of interest.

References

1. B.P. Hallbert, J. Persensky, C. Smidts et al., in the light water reactor sustainability workshop on advanced instrumentation, information, and control systems and human-system interface technologies, Idaho National Lab(INL), Idaho Falls (ID. United States (2009). https://doi.org/10.2172/974785
2. E. Blain, Measurement of prompt fission neutron spectrum using a gamma tag double time-of-flight setup, Rensselaer Polytechnic Institute, 2014
3. A. Klein and J. Lance, Future Directions, Challenges and Opportunities in Nuclear Energy, (American Institute of Physics, 2007)
4. Z.Q. Chen, Recent progress in nuclear data measurement for ADS at IMP. Nucl. Sci. Tech. **28**, 184 (2017). https://doi.org/10.1007/s41365-017-0335-3
5. B. Zhang, X. Ma, K. Hu et al., Performance of the CENDL-3.2 and other major neutron data libraries for criticality calculations. Nucl. Sci. Tech. **33**, 8 (2022). https://doi.org/10.1007/s41365-022-00994-3
6. C. Wulandari, A. Waris, S. Permana et al., Evaluating the JEFF 3.1, ENDF/B-VII.0, JENDL 3.3, and JENDL 4.0 nuclear data libraries for a small 100 MWe molten salt reactor with plutonium fuel. Nucl. Sci. Tech. **33**, 165 (2022). https://doi.org/10.1007/s41365-022-01141-8
7. Y. Chen, R. Liu, H. Guo et al., Neutronics intergral experiments. Trends. Nucl. Phys. **54**, 12 (1995)
8. S. Duan, Measurement of Tritium Production in ^{6}LiD irradiated with neutrons from a critical system. China Nuclear Science and Technology Report, 51(1998). (In Chinese)
9. S. Duan,The measurement of tritium produced in a ^{6}LiD sphere irradiated by neutrons from D-D and ^{252}Cf. China Nuclear Science and Technology Report, 486 (1997) (In Chinese)
10. R. Liu, T. Zhu, L. An et al., Reaction rates in blanket assemblies of a fusion-fission hybrid reactor. Nucl. Sci. Tech. **23**, 242 (2012). https://doi.org/10.13538/j.1001-8042/nst.23.242-246
11. Y. Chen, H. Guo and X. Yan et al., Neutronics experiment of vanadium shell benchmark with14 MeV neutron source. Atomic Energy Sci. Technol. **36**, 157 (2002). (in Chinese)
12. Y. Nie, J. Ren, X. Ruan et al., Benchmark experiments with slab sample using time-of-flight technique at CIAE. Ann. Nucl. Energy **136**, 107040 (2020). https://doi.org/10.1016/j.anucene.2019.107040
13. Y. Ding, Y. Nie, J. Ren et al., Benchmark experiment for bismuth by slab samples with DT neutron source. Fusion Eng. Des. **167**, 112312 (2021). https://doi.org/10.1016/j.fusengdes.2021.112312
14. Y. Ding, Y. Nie, Y. Zhang et al., Benchmark experiment on slab ^{238}U with DT neutrons for validation of evaluated nuclear data. Nucl. Sci. Tech. **35**, 29 (2024). https://doi.org/10.1007/s41365-024-01386-5
15. Q. Zhao, Y. Nie, Y. Ding et al., Measurement and simulation of the leakage neutron spectra from Fe spheres bombarded with 14 MeV neutrons. Nucl. Sci. Tech. **34**, 182 (2023). https://doi.org/10.1007/s41365-023-01329-6
16. S. Zhang, Y.B. Nie, J. Ren et al., Benchmarking of JEFF-3.2, FENDL-3.0 and TENDL-2014 evaluated data for tungsten with 148 MeV neutrons. Nucl. Sci. Tech. **27**, 28 (2017). https://doi.org/10.1007/s41365-017-0192-0
17. R. Han, Z. Chen, Y. Nie et al., Measurement and analysis of leakage neutron spectra from lead slab samples with D-T neutrons. Appl. Radiat. Isot. **203**, 111113 (2024). https://doi.org/10.1016/j.apradiso.2023.111113
18. S. Zhang, D. Niu, D. Wang et al., Measurement of leakage neutron spectra for aluminium with DT fusion neutrons and validation of evaluated nuclear data. Fusion Eng. Des. **171**, 112582 (2021). https://doi.org/10.1016/j.fusengdes.2021.112582
19. H. Werle, H. Bluhm, Fission-neutron spectra measurements of ^{235}U, ^{239}Pu and ^{252}Cf. J. Nucl. Energy **4**, 26 (1972). https://doi.org/10.1016/0022-3107(72)90025-1
20. E. Blain, A. Daskalakis, R.C. Block et al., Measurement of prompt fission neutron spectrum for spontaneous fission of ^{252}Cf using γ multiplicity tagging. Phys. Rev. C **95**, 064615 (2017). https://doi.org/10.1103/PhysRevC.95.064615
21. B. Devkin, M. Kobozev, S. Simakov et al., Neutron leakage spectra from iron spheres with ^{252}Cf neutron source. Institutfur Neutronenphysik und Reaktortechnik. (Germany, 1998)
22. B. Janské, E. Novak, Z. Turzík et al., Neutron and gamma spectra measurements and calculations in benchmark spherical iron assemblies with ^{252}Cf neutron source in the centre. Nucl. Instrum. Meth. A. **476**, 358–364 (2002). https://doi.org/10.1016/S0168-9002(01)01470-X
23. M. Schulc, M. Koál, E. Novák et al., Application of ^{252}Cf neutron source for precise nuclear data experiments. Appl. Radiat. Isot. **187**, 151 (2019). https://doi.org/10.1016/j.apradiso.2019.06.012
24. M. Schulc, M. Koál, E. Novák et al., Measuring neutron leakage spectra using spherical benchmarks with ^{252}Cf source in its centers. Nucl. Instrum. Meth. A. **53**, 914 (2019). https://doi.org/10.1016/j.nima.2018.10.164
25. J. F. Briesmeister, MCNPTM-A general Monte Carlo N-particle transport code. Version 4C, LA-13709-M, Los Alamos National Laboratory. **2** (2000)
26. D.A. Brown, M. Chadwick, R. Capote et al., ENDF/B-VIII. 0: the 8th major release of the nuclear reaction data library with CIELO-project cross sections, new standards and thermal scattering data. Nucl. Data. Sheets. **148**, 1–142 (2018). https://doi.org/10.1016/j.nds.2018.02.001
27. Z. Ge, R. Xu, H. Wu et al., CENDL-3.2: The new version of Chinese general purpose evaluated nuclear data library. EPJ Web of Conf. **239** , 09001(2020). https://doi.org/10.1051/epjconf/202023909001
28. O. Cabellos, F. Alvarez-Velarde, M. Angelone et al., Benchmarking and validation activities within JEFF project. EPJ Web of

Conf. **146**, 06004 (2017). https://doi.org/10.1051/epjconf/201714606004
29. O. Iwamoto, N. Iwamoto, S. Kunieda et al., Japanese evaluated nuclear data library version 5: JENDL-5. J. Nucl. Sci. Technol. **60**, 1 (2023). https://doi.org/10.1080/00223131.2022.2141903
30. K. Li, X. Zhang, Q, Guiet al., Characterization of the new scintillator Cs_2LiYCl_6: Ce^{3+}. Nucl. Sci. Tech. **29**, 11 (2018). https://doi.org/10.1007/s41365-017-0342-4
31. A. Giaz, L. Pellegri, F. Camera et al., The CLYC-6 and CLYC-7 response to γ-rays, fast and thermal neutrons. Nucl. Instrum. Methods Phys. Res. A **132**, 810 (2016). https://doi.org/10.1016/j.nima.2015.11.119
32. Z. Ren, B. Hu, Z. Zhao et al., Digital coincidence acquisition applied to portable beta liquid scintillation counting device. Nucl. Sci. Tech. **24**, 3 (2013). https://doi.org/10.13538/j.1001-8042/nst.2013.03.012
33. E. Blain, A. Daskalakis, R. Block et al., A method to measure prompt fission neutron spectrum using gamma multiplicity tagging. Nucl. Instrum. Methods Phys. Res. A **95**, 805 (2016). https://doi.org/10.1016/j.nima.2015.08.060
34. G. Dietze and H. Klein, NRESP4 and NEFF4-Monte Carlo codes for the calculation of neutron response functions and detection efficiencies for NE213 scintillation detectors. (1982)
35. Q. Zhao, Y. Nie, Y. Ding et al., Measurement and Calculation of Leakage Neutron and γ Spectra from Bi Slab Sample. Atomic Energy Sci. Technol. **584**, 55 (2021) (In Chinese). https://doi.org/10.7538/yzk.2020.youxian.0438
36. D. Cester, M. Lunardon, G. Nebbia et al., Pulse shape discrimination with fast digitizers. Nucl. Instrum. Methods Phys. Res. A **33**, 748 (2014). https://doi.org/10.1016/j.nima.2014.02.032
37. F. Ferrulli, M. Labalme, M. Silari, Investigation of CLYC-6 for thermal neutron detection and CLYC-7 for fast neutron spectrometry. Nucl. Instrum. Methods Phys. Res. A **1029**, (2022). https://doi.org/10.1016/j.nima.2022.166460
38. C. Wagemans, *The Nuclear Fission Process* (CRC Press, Boca Raton, Ann Arbor, Boston, London, Cyriel Wagemans, 1991)
39. J. W. Boldeman, IAEA-TECDOC-410 125, 1987
40. F. Becchetti, M. Febbraro, R. Torres-Isea et al., ^{252}Cf fission-neutron spectrum using a simplified time-of-flight setup: An advanced teaching laboratory experiment. Am. J. Phys. **112**, 81 (2013). https://doi.org/10.1119/1.4769032
41. A.J. Grievson, Time-of-Flight Spectrometry of the Spontaneous Fission Neutron Emission of ^{244}Cm and ^{252}Cf Using EJ-309 Liquid Scintillators (Lancaster University, United Kingdom, 2020)
42. H. Maier-Leibnitz, P. Armbruster, H.J. Specht et al., *Prompt and delayed gamma-rays from fission* (Phys. Chem. Fission, Salzburg, Austria, 1965)
43. National Nuclear Data Center. https://www.nndc.bnl.gov/endf/